# $e^- - e^+$ pair creation by vacuum polarization around electromagnetic black holes

C. Cherubini,[1,2] A. Geralico,[1,3] J. A. Rueda H.,[1,3] and R. Ruffini[1,3,*]

[1]*ICRANet, I-65100 Pescara, Italy*
[2]*Nonlinear Physics and Mathematical Modeling Lab, C.I.R., University Campus Bio-Medico, I-00128 Rome, Italy*
[3]*Physics Department and ICRA, University of Rome "La Sapienza", I-00185 Rome, Italy*
(Received 12 January 2009; published 3 June 2009)

The concept of "dyadotorus" was recently introduced to identify in the Kerr-Newman geometry the region where vacuum polarization processes may occur, leading to the creation of $e^- - e^+$ pairs. This concept generalizes the original concept of "dyadosphere" initially introduced for Reissner-Nordström geometries. The topology of the axially symmetric dyadotorus is studied for selected values of the electric field and its electromagnetic energy is estimated by using three different methods all giving the same result. It is shown by a specific example the difference between a dyadotorus and a dyadosphere. The comparison is made for a Kerr-Newman black hole with the same total mass energy and the same charge to mass ratio of a Reissner-Nordström black hole. It turns out that the Kerr-Newman black hole leads to larger values of the electromagnetic field and energy when compared to the electric field and energy of the Reissner-Nordström one. The significance of these theoretical results for the realistic description of the process of gravitational collapse leading to black hole formation as well as the energy source of gamma ray bursts are also discussed.

## I. INTRODUCTION

Relativistic astrophysics differs from the other branches of physics and astronomy by exploring new fundamental processes unprecedented for the spectacularly large scales of the involved observables and for their extremely short time variability. Following the well-known case of supernova with energies $\lesssim 10^{53}$ ergs on time scales of months, gamma-ray bursts (GRBs) have offered an extreme example of the most energetic ($E \lesssim 10^{55}$ ergs) and the fastest transient ($\Delta t \lesssim 10^{-3}$–$10^4$ s) phenomena ever observed in the universe [1]. The dynamics of GRBs is dominated by an electron-positron plasma [2]. The theoretical model based on the vacuum polarization processes [3] occurring in a Kerr-Newman geometry [4] can indeed explain such enormous energetics and the sharp time variability. What is most important is that such a model is based on explicit analytic solutions of well-tested ultrarelativistic field theories. The formation of such black holes in a process of gravitational collapse is expected from a large variety of binary mergers composed of neutron stars, white dwarfs, and massive stars at the end point of their thermonuclear evolution [5] in all possible combinations.

In particular, in the merging of two neutron stars and in the final process of gravitational collapse to a black hole is expected the occurrence of electromagnetic fields with strength larger than the critical value of vacuum polarization

$$E_c = \frac{m_e^2 c^3}{\hbar e},\tag{1}$$

where $m_e$ and $e$ are the electron mass and charge, respectively [1]. We are currently reexamining the electrodynamical processes of a neutron star via an ultrarelativistic Thomas-Fermi equation to identify the possible physical origin of this overcritical electric field [6–8].

The time evolution of the gravitational collapse (occurring on characteristic gravitational time scales $\tau = GM/c^3 \simeq 5 \times 10^{-5} M/M_\odot$ s) and the associated electrodynamical process are too complex for a direct description. We address here a more confined problem: the polarization process around an already formed Kerr-Newman black hole. This is a well-defined theoretical problem which deserves attention. It may represent a physical state asymptotically reached in the process of gravitational collapse. We expect such an asymptotic configuration be reached when all the multipoles departing from the Kerr-Newman geometry have been radiated away either by process of vacuum polarization or electromagnetic and gravitational waves. What is most important is that by performing this theoretical analysis we can gain a direct evaluation of the energetics of the spectra and dynamics of the $e^- - e^+$ plasma created on the extremely short time scales due to the quantum phenomena of $\Delta t = \hbar/(m_e c^2) \simeq 10^{-21}$ s. This entire transient phenomena, starting from an initial neutral condition, undergoes the formation of the Kerr-Newman black hole by the collective effects of gravitation, strong, weak, electromagnetic interactions during a fraction of the above-mentioned gravitational characteristic time scale of collapse.

The aim of this article is to explore the initial condition for such a process to occur using the recently introduced concept of "dyadotorus" [4] which generalizes to the Kerr-Newman geometry the concept of the "dyadosphere"

*ruffini@icra.it

previously introduced in the case of the spherically symmetric Reissner-Nordström geometry [9,10].

Damour and Ruffini [3] showed that vacuum polarization processes *à la* Sauter-Heisenberg-Euler-Schwinger [11–13] can occur in the field of a Kerr-Newman black hole endowed with a mass ranging from the maximum critical mass for neutron stars $(3.2 M_\odot)$ all the way up to $7.2 \times 10^6 M_\odot$. It is an almost perfectly reversible process in the sense defined by Christodoulou and Ruffini [14], leading to a very efficient mechanism of extracting energy from the black hole.

In the case of absence of rotation in spacetime, we have a Reissner-Nordström black hole as the background geometry. The region where vacuum polarization processes take place is a sphere centered about the hole, and has been called dyadosphere [9,10]. Its main properties are recalled in Sec. II.

We investigate in Sec. III how the presence of rotation in spacetime modifies the shape of the surface containing the region where electron-positron pairs are created. Because of the axial symmetry we call that region dyadotorus and we give the conditions for its existence. We then provide some pictorial representations of the boundary surface of the dyadotorus by using the Boyer-Lindquist radial and angular coordinates as polar coordinates in flat space as well as by employing Kerr-Schild coordinates. We show in Sec. IV the dyadotorus on the corresponding embedding diagrams, which reveal the intrinsic structure of the spacetime geometry. In Sec. V we provide an estimate of the electromagnetic energy contained in the dyadotorus by using three different definitions commonly adopted in the literature, i.e. the standard definition in terms of the time-like Killing vector (see e.g. [15]), the one recently suggested by Katz, Lynden-Bell and Bičák [16,17] for axially symmetric asymptotically flat spacetimes, which is an observer dependent definition of energy, and the last one involving the theory of pseudotensors (see e.g. [18]). All these approaches are shown to give the same results. Finally, a comparison is made between the electromagnetic energy of an extreme Kerr-Newman black hole and the corresponding one of a Reissner-Nordström black hole with the same total mass and charge to mass ratio. In addition to the topological differences between the dyadotorus and the dyadosphere, it is shown how larger field strengths are allowed in the case of a Kerr-Newman geometry close to the horizon, when compared with a Reissner-Nordström black hole of the same mass energy and charge to mass ratio.

We finally draw some general conclusions.

## II. THE DYADOSPHERE

In this section we recall the definition of dyadosphere and its main properties in the field of a Reissner-Nordström black hole as derived in [9,10]. In standard Schwarzschild-like coordinates the Reissner-Nordström black hole metric is given by

$$ds^2 = -\left(1 - \frac{2M}{r} + \frac{Q^2}{r^2}\right)dt^2 + \left(1 - \frac{2M}{r} + \frac{Q^2}{r^2}\right)^{-1}dr^2 + r^2(d\theta^2 + \sin^2\theta d\phi^2), \tag{2}$$

where geometric units $G = c = 1$ have been adopted. The associated electromagnetic field is given by

$$F = -\frac{Q}{r^2}dt \wedge dr. \tag{3}$$

The horizons are located at $r_\pm = M \pm \sqrt{M^2 - Q^2}$; we consider the case $|Q| \le M$ and the region $r > r_+$ outside the outer horizon. For an extremely charged hole we have $|Q| = M$ and the two horizons coalesce.

Let us introduce an orthonormal frame adapted to the static observers

$$e_{\hat{t}} = \left(1 - \frac{2M}{r} + \frac{Q^2}{r^2}\right)^{-1/2}\partial_t,$$

$$e_{\hat{r}} = \left(1 - \frac{2M}{r} + \frac{Q^2}{r^2}\right)^{1/2}\partial_r, \tag{4}$$

$$e_{\hat{\theta}} = \frac{1}{r}\partial_\theta, \qquad e_{\hat{\phi}} = \frac{1}{r\sin\theta}\partial_\phi.$$

The electric field as measured by static observers with four-velocity $U = e_{\hat{t}}$ is purely radial:

$$E(U) = \frac{Q}{r^2}e_{\hat{r}}. \tag{5}$$

The radius $r_{\mathrm{ds}}$ at which the electric field strength $|\mathbf{E}| = |E^{\hat{r}}|$ reaches the critical value $E_c$ has been defined in [9,10] as the outer radius of the dyadosphere, which extends down to the horizon and within which the electric field strength exceeds the critical value,

$$r_{\mathrm{ds}} \simeq 1.12 \times 10^8\sqrt{\lambda\mu} \text{ cm}, \tag{6}$$

where the dimensionless quantities $\lambda = Q/M$ and $\mu = M/M_\odot$ have been introduced. The critical electric field (1) in geometric units is given by $E_c \approx 1.268 \times 10^{-11} \text{ cm}^{-1}$.

The electromagnetic energy contained inside the dyadosphere has been evaluated by Vitagliano and Ruffini [15],

$$E(\xi)_{(r_+,r_{\mathrm{ds}})} = \frac{Q^2}{2r_+}\left(1 - \frac{r_+}{r_{\mathrm{ds}}}\right), \tag{7}$$

by using a "truncated version" of the definition of energy in terms of the conserved Killing integral,

$$E(\xi) = \int_\Sigma T_{\mu\nu}^{(\mathrm{em})}\xi^\mu d\Sigma^\nu, \tag{8}$$

where $\xi = \partial_t$ is the timelike Killing vector. We refer to Sec. V for a detailed discussion on this point. Figure 1 shows the behavior of the electromagnetic energy (7) as a
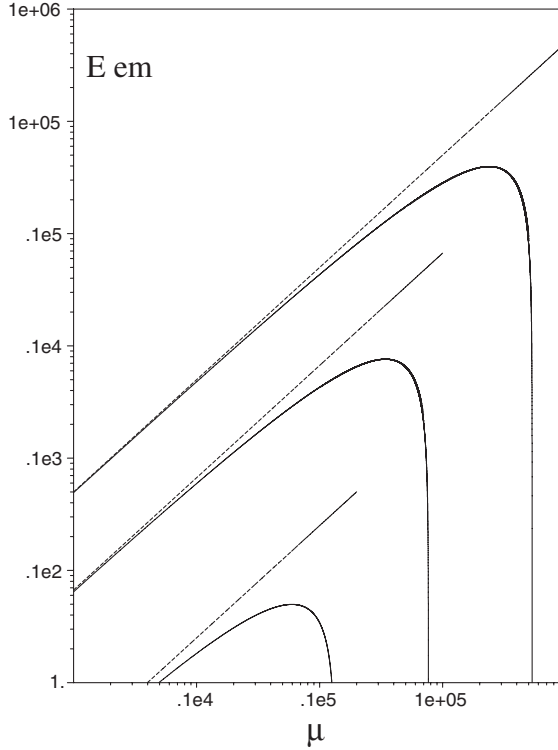
FIG. 1. The behavior of the electromagnetic energy (7) in solar mass units is shown as a function of the mass parameter $\mu$ for selected values of the charge parameter $\lambda = [0.1, 0.5, 1]$, from bottom to top. The straight lines (dashed) correspond to the maximum energy extractable from a Reissner-Nordström black hole given by $Q^2/(2r_+)$.

function of the mass parameter $\mu$ for fixed values of the charge parameter $\lambda$.

Ruffini and collaborators estimated also the total energy of pairs converted from the "static electric energy" (7) and deposited within the dyadosphere:

$$E_{\text{pairs}} = \frac{Q^2}{2r_+}\left(1 - \frac{r_+}{r_{\text{ds}}}\right)\left[1 - \left(\frac{r_+}{r_{\text{ds}}}\right)^4\right]. \tag{9}$$

Its behavior as a function of the charge and mass parameters $\lambda$ and $\mu$ is shown in Fig. 2.

The rate of pair creation per unit four-volume is given by the Schwinger formula [13]:

$$2\,\text{Im}\mathcal{L} = \frac{1}{4\pi}\left(\frac{|\mathbf{E}|e}{\pi\hbar}\right)^2 \sum_{n=1}^{\infty} \frac{1}{n^2} e^{-n\pi E_c/|\mathbf{E}|}. \tag{10}$$

The leading term $n = 1$ agrees with the WKB results obtained by Sauter [11] and Heisenberg-Euler [12]:

$$2\,\text{Im}\mathcal{L} = \frac{1}{4\pi}\left(\frac{|\mathbf{E}|e}{\pi\hbar}\right)^2 e^{-\pi E_c/|\mathbf{E}|}. \tag{11}$$

The dyadosphere has been defined by Ruffini and collaborators [9,10] by the condition $|\mathbf{E}| = E_c$. One might better define it by requiring the electric field strength to be
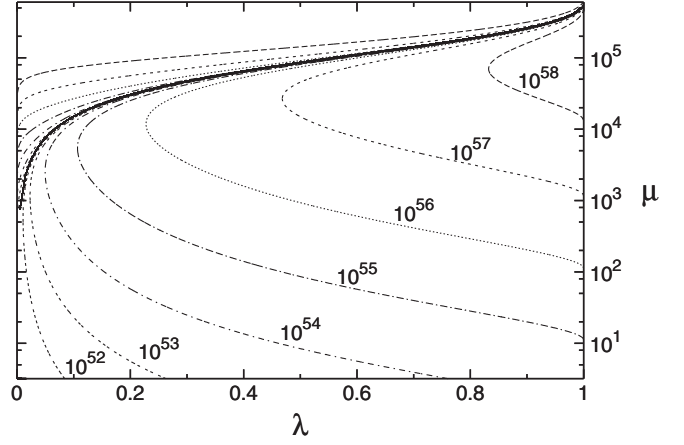


FIG. 2. The total energy of pairs (9) is plotted as a function of the two mass and charge parameters $\mu$ and $\lambda$. The different curves correspond to selected values of the energy (in ergs). Only the solutions below the solid line are physically relevant. The configurations above the solid line correspond instead to unphysical solutions with $r_{\text{ds}} < r_+$. The plot is reproduced from [33] with the kind permission of the authors.

such that the rate of pair creation is suppressed exactly by a factor $1/e$, leading to the condition $|\mathbf{E}| = \pi E_c$. However, from Eq. (10) it is clear that no sharp threshold exists for electron-positron pair creation, so that the definition

$$|\mathbf{E}| = kE_c \tag{12}$$

appears to be more appropriate and should be explored for different values of the constant parameter $k$, even for $k < 1$. Consequently, we shall define in the following both dyadosphere and dyadotorus as the locus of points where the electric field satisfies the condition (12).

## III. THE DYADOTORUS

The Kerr-Newman metric in standard Boyer-Linquist–type coordinates writes as [19]

$$ds^2 = -\left(1 - \frac{2Mr - Q^2}{\Sigma}\right)dt^2 - \frac{2a\sin^2\theta}{\Sigma}(2Mr - Q^2)dtd\phi$$

$$+ \frac{\Sigma}{\Delta}dr^2 + \Sigma d\theta^2$$

$$+ \left[r^2 + a^2 + \frac{a^2\sin^2\theta}{\Sigma}(2Mr - Q^2)\right]\sin^2\theta d\phi^2, \tag{13}$$

with associated electromagnetic field

$$F = \frac{Q}{\Sigma^2}(r^2 - a^2\cos^2\theta)dr \wedge [dt - a\sin^2\theta d\phi]$$

$$+ 2\frac{Q}{\Sigma^2}ar\sin\theta\cos\theta d\theta \wedge [(r^2 + a^2)d\phi - adt], \tag{14}$$

where $\Sigma = r^2 + a^2\cos^2\theta$ and $\Delta = r^2 - 2Mr + a^2 + Q^2$. Here $M$, $Q$, and $a$ are the total mass, total charge, and

specific angular momentum, respectively, characterizing the spacetime. The (outer) event horizon is located at $r_+ = M + \sqrt{M^2 - a^2 - Q^2}$.

Let us introduce the Carter's observer family [20], whose four-velocity is given by

$$U_{\text{car}} = \frac{r^2 + a^2}{\sqrt{\Delta\Sigma}}\left[\partial_t + \frac{a}{r^2 + a^2}\partial_\phi\right]. \quad (15)$$

An observer adapted frame to $U_{\text{car}}$ is then easily constructed with the triad

$$e_{\hat{r}} = \frac{1}{\sqrt{g_{rr}}}\partial_r, \qquad e_{\hat{\theta}} = \frac{1}{\sqrt{g_{\theta\theta}}}\partial_\theta,$$
$$\bar{U}_{\text{car}} = \frac{a\sin\theta}{\sqrt{\Sigma}}\left[\partial_t + \frac{1}{a\sin^2\theta}\partial_\phi\right]. \quad (16)$$

The Carter observers measure parallel electric and magnetic fields $E$ and $B$ [3], with components

$$E(U_{\text{car}})^\alpha = F^\alpha{}_\beta U^\beta_{\text{car}}, \qquad B(U_{\text{car}})^\alpha = {}^*F^\alpha{}_\beta U^\beta_{\text{car}}, \quad (17)$$

where $^*F$ is the dual of the electromagnetic field (14). Both $E$ and $B$ are directed along $e_{\hat{r}}$ and assuming as usual $Q > 0$, the strength of electric and magnetic fields is given by

$$|\mathbf{E}| = |E^{\hat{r}}| = \frac{Q}{\Sigma^2}(r^2 - a^2\cos^2\theta),$$
$$|\mathbf{B}| = |B^{\hat{r}}| = \left|2\frac{Q}{\Sigma^2}ar\cos\theta\right|. \quad (18)$$

It is worth noting that the Carter orthonormal frame is the unique frame in which the flat spacetime Schwinger discussion can be locally applied. This is due both to the meaning of the Carter orthonormal frame and its relation to the geometry of the Weyl curvature tensor and the spacetime itself, as well as to the fact that the invariantly described Schwinger process demands this unique frame for its application. An alternative but equivalent derivation of this result is presented in Appendix A, where the electric and magnetic field strengths are obtained in terms of the electromagnetic invariants by using the Newman-Penrose formalism, hence showing more clearly the invariant character of the dyadotorus.

The Schwinger formula generalized to include both electric and magnetic fields, i.e.,

$$2\,\text{Im}\mathcal{L} = \frac{1}{4\pi}\left(\frac{|\mathbf{E}|e}{\pi\hbar}\right)^2\sum_{n=1}^\infty\frac{1}{n^2}\left(n\pi\frac{|\mathbf{B}|}{|\mathbf{E}|}\right)$$
$$\times\coth\left(n\pi\frac{|\mathbf{B}|}{|\mathbf{E}|}\right)e^{-n\pi E_c/|\mathbf{E}|}, \quad (19)$$

has been used by Damour and Ruffini [3] for the case of a Kerr-Newman geometry.

We are interested in the region exterior to the outer horizon $r \geq r_+$. Solving Eq. (12) for $r$ and introducing the dimensionless quantities $\lambda = Q/M$, $\alpha = a/M$, $\mu = M/M_\odot$, and $\epsilon = kE_cM_\odot \approx 1.873k \times 10^{-6}$ (with $M_\odot \approx 1.477 \times 10^5$ cm), we get

$$\left(\frac{r^d_\pm}{M}\right)^2 = \frac{1}{2}\frac{\lambda}{\mu\epsilon} - \alpha^2\cos^2\theta \pm \left[\frac{1}{4}\frac{\lambda^2}{\mu^2\epsilon^2} - 2\frac{\lambda}{\mu\epsilon}\alpha^2\cos^2\theta\right]^{1/2}, \quad (20)$$

where the $\pm$ signs correspond to the two different parts of the surface. They join at the particular values $\theta^*$ and $\pi - \theta^*$ of the polar angle given by the condition of vanishing argument of the square root in Eq. (20):

$$\theta^* = \arccos\left(\frac{1}{2\sqrt{2}\alpha}\sqrt{\frac{\lambda}{\mu\epsilon}}\right). \quad (21)$$

The requirement that $\cos\theta^* \leq 1$ can be solved for instance for the constant parameter $k$, giving the range of allowed values for which the dyadotorus appears indeed as a torus-like surface [see Figs. 4(b)–4(d)]:
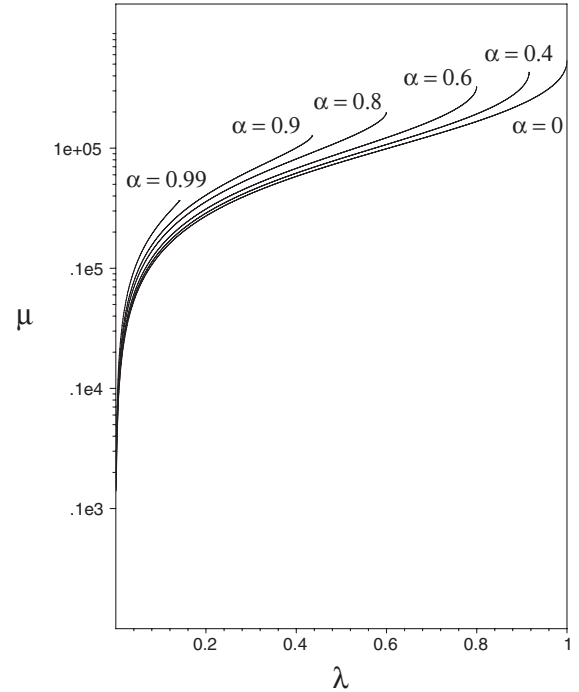


FIG. 3. The space of parameters $(\lambda, \mu)$ is shown for different values of the rotation parameter $\alpha = a/M = [0, 0.4, 0.6, 0.8, 0.9, 0.99]$ and fixed value of the polar angle $\theta = \pi/3$. The region below each curve represents the allowed region for the existence of the dyadoregion with fixed $\alpha$. The configurations above each line correspond to unphysical solutions where $r^d_\pm < r_+$ for the selected set of parameters. The value of the parameter $k$ has been set equal to one.
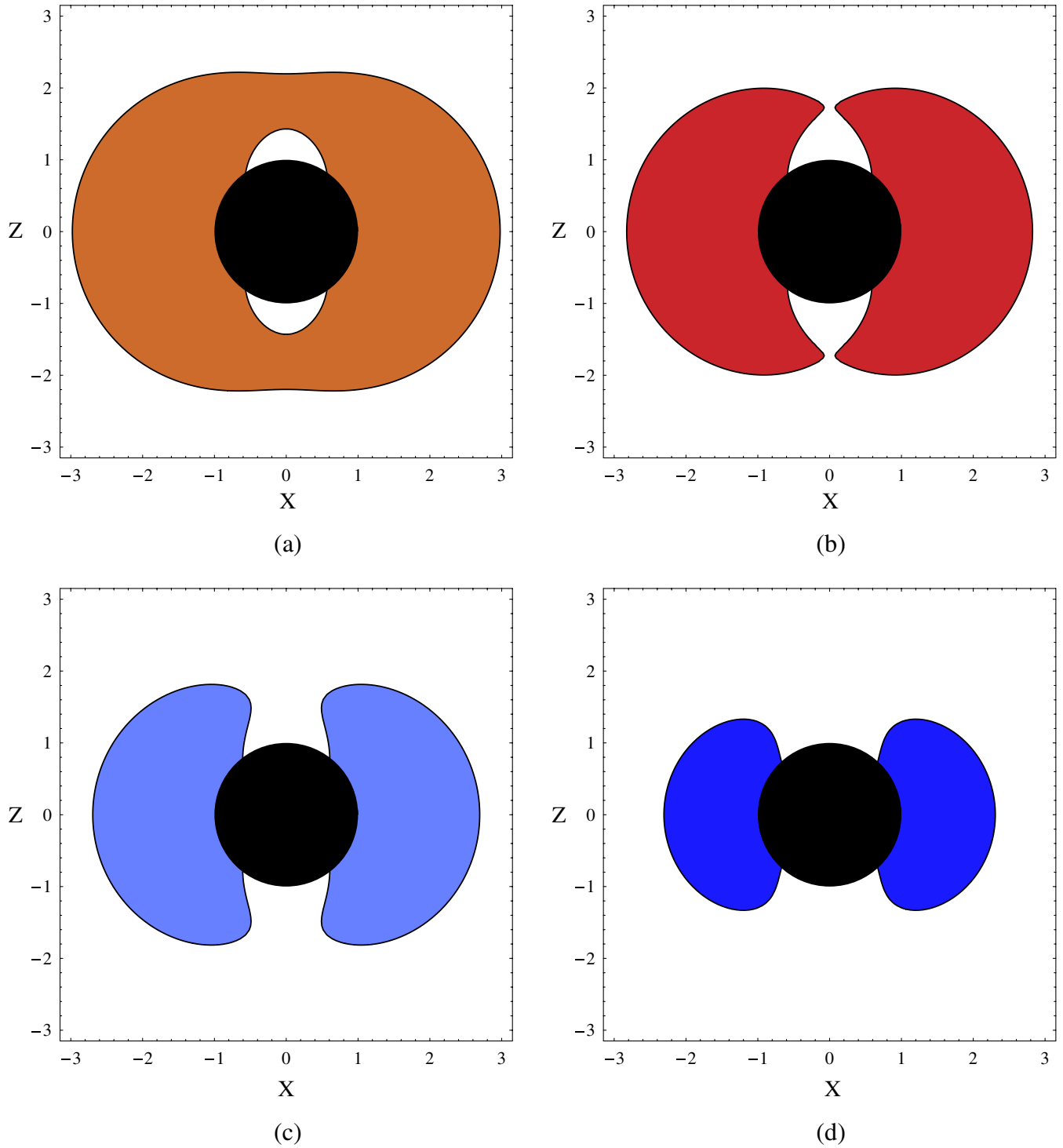
FIG. 4 (color online). The projection of the dyadotorus on the $X - Z$ plane ($X = r \sin\theta$, $Z = r \cos\theta$ are Cartesian-like coordinates built up simply using the Boyer-Lindquist radial and angular coordinates) is shown for an extreme Kerr-Newman black hole with $\mu = 10$, $\lambda = 1.49 \times 10^{-4}$, and different values of the parameter $k$: (a) $k = 0.9$ (orange), (b) $k = 1.0$ (red), (c) $k = 1.1$ (light blue), (d) $k = 1.5$ (blue). The boundary of the dyadoregion becomes a toruslike surface for $k \approx 0.998$, according to Eq. (22). The black disk represents the black hole horizon.

$$k \geq \frac{\lambda}{8 E_c M_\odot \mu \alpha^2} \approx 6.6 \times 10^4 \frac{\lambda}{\mu \alpha^2}; \qquad (22)$$

for lower values of $k$ the dyadotorus consists instead of two disjoint parts, one of them (corresponding to the branch $r_+^d$) always external to the other (corresponding to the

branch $r_-^d$), and has rather the shape of an ellipsoid [see Fig. 4(a)]. Therefore, the use of the term dyadoregion should be more appropriate in this case.

In terms of the dimensionless quantities $\lambda$ and $\alpha$ the horizon radius is then given by

$$\frac{r_+}{M} = 1 + \sqrt{1 - \lambda^2 - \alpha^2}. \tag{23}$$

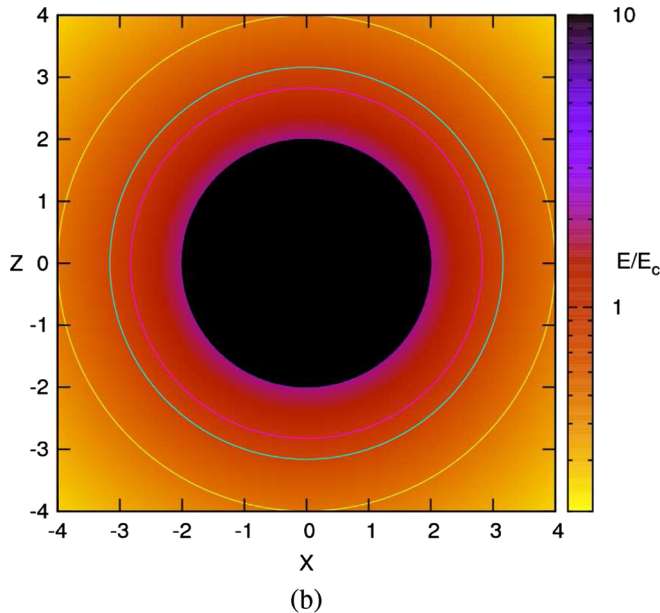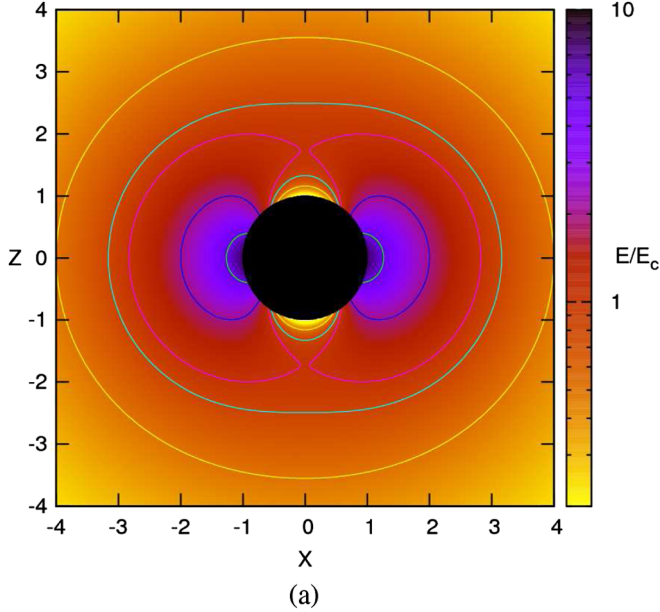The condition for the existence of the dyadotorus is given



(a)



(b)

FIG. 5 (color online). The projections of the dyadotorus on the $X - Z$ plane corresponding to different values of the ratio $|\mathbf{E}|/E_c \equiv k$ are shown in (a) for $\mu = 10$ and $\lambda = 1.49 \times 10^{-4}$. The corresponding plot for the dyadosphere with the same mass energy and charge to mass ratio is shown in (b) for comparison.

by $r_\pm^d \geq r_+$. The allowed region for the pairs $(\lambda, \mu)$ (with fixed values of the rotation parameter $\alpha$ and the polar angle $\theta$) satisfying this condition is shown in Fig. 3.

Figure 4 shows the shape of the projection of the dyadotorus on a plane containing the rotation axis for an extreme Kerr-Newman black hole with fixed $\mu$ and $\lambda$ and different values of the parameter $k$ using Cartesian-like coordinates $X = r \sin\theta$, $Z = r \cos\theta$, built up simply by taking the Boyer-Lindquist coordinates $r$ and $\theta$ as polar coordinates in flat space.

A "dynamical" view of topology change in the shape of the dyadoregion is shown in Fig. 5, where the case of a Reissner-Nordström black hole with the same total mass and charge is also shown for comparison. We point out some interesting qualitative differences between dyadotorus and dyadosphere which can be seen clearly from these plots. In particular, the dyadotorus appear to lead to larger values of the electric field than the corresponding dyadosphere close to the horizon. A key point here is the size of the horizon, which in the limit of small charge to mass ratio $\lambda \ll 1$ for an extreme Kerr-Newman black hole goes to $r_+ \sim M$, while in the case of a Reissner-Nordström black hole goes to $r_+ \sim 2M$. This fact is crucial because it leads to the presence of stronger electric fields for the Kerr-Newman black hole in contrast with the Reissner-Nordström one. We can compare for instance the maximum electric field $E_{max} = Q/r_+^2$ of an extreme Kerr-Newman black hole and of a Reissner-Nordström black hole, which is obtained for $r = r_+$, $\theta = \pi/2$ in the former case and $r = r_+$ in the latter case, in the limit of small charge to mass ratio

$$E_{max}^{KN} = \frac{Q}{M^2} = 4E_{max}^{RN}. \tag{24}$$

We will turn to the energetics of the dyadoregion in Sec. V.

Three-dimensional images of the dyadotorus can be generated also in terms of Kerr-Schild coordinates $(\tilde{t}, x, y, z)$, which are related to the standard Boyer-Lindquist ones $(t, r, \theta, \phi)$ by the equations (see e.g. [19])

$$\begin{aligned} d\tilde{t} &= dt - \frac{2Mr - Q^2}{\Delta} dr, \\ d\psi &= d\phi - \frac{a}{r^2 + a^2} \frac{2Mr - Q^2}{\Delta} dr, \\ x &= \sqrt{r^2 + a^2} \sin\theta \cos\psi, \\ y &= \sqrt{r^2 + a^2} \sin\theta \sin\psi, \\ z &= r \cos\theta. \end{aligned} \tag{25}$$

Note that the spatial coordinates $(x, y, z)$ satisfy the relation

$$\frac{x^2 + y^2}{r^2 + a^2} + \frac{z^2}{r^2} = 1, \tag{26}$$

and the auxiliary angular coordinate $\psi$ is a function of $r$, as from the second relation of Eq. (25)

$$\psi = \phi - \int^r \frac{a}{r^2 + a^2} \frac{2Mr - Q^2}{\Delta} dr. \qquad (27)$$

The shape of the dyadotorus using Kerr-Schild coordinates is shown in Fig. 6 for the same choice of parameters as in Fig. 4.

## IV. EMBEDDING DIAGRAM

The plots of Figs. 4 and 6 actually show a distorted view of the shape of the dyadotorus; we should rather look at the corresponding embedding diagram, which gives the correct geometry allowing to visualize the spacetime curvature. Because of our familiar three-dimensional intuition, the most useful and easily understood embedding diagrams
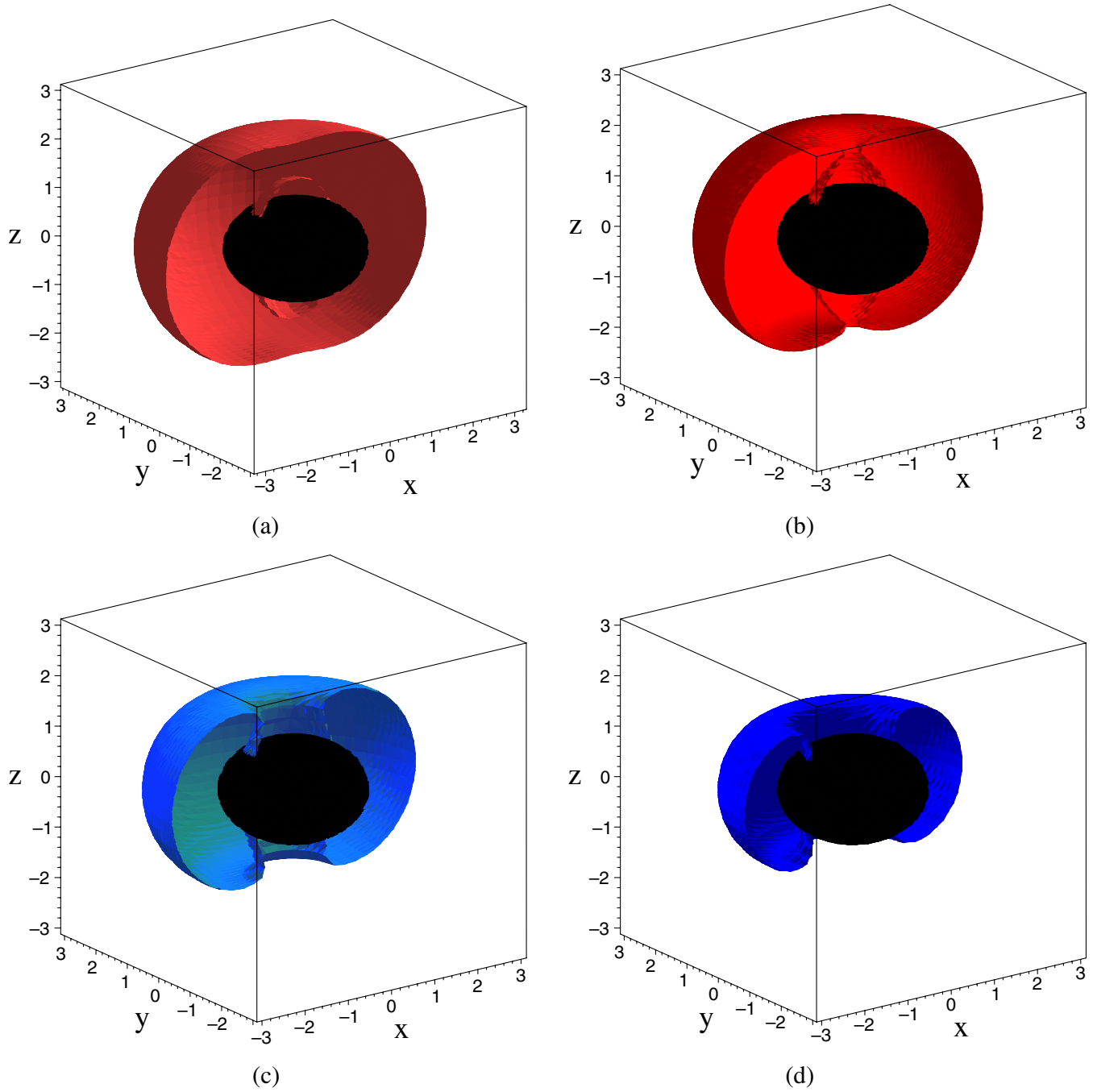


(a)

(b)

(c)

(d)

FIG. 6 (color online).   Three-dimensional images of the dyadotorus are shown using Kerr-Schild coordinates. The parameter choice is the same as in Fig. 4. The surfaces have been cut in half for a better view of the interior. The horizon instead has been shown entirely (black region).

are those which take a Riemannian two-surface from the original geometry, then reconstructing it as a distorted surface in a three-dimensional Euclidean space.

The dyadotorus implicitly defined by Eq. (20) can be visualized as a two-dimensional surface of revolution around the rotation axis embedded in the usual Euclidean 3-space by suppressing the temporal and azimuthal dependence. Using Boyer-Lindquist coordinates, from Eq. (13) we get the following induced metric of the constant time slice ($dt = 0$) of the world sheet $r = r^d_\pm$ given by Eq. (20):

$$^{(2)}ds^2 = h_{\eta\eta}d\eta^2 + g_{\phi\phi}d\phi^2,$$
$$h_{\eta\eta} = g_{rr}\left(\frac{dr^d_\pm}{d\eta}\right)^2 + \frac{g_{\theta\theta}}{1 - \eta^2}, \tag{28}$$

where $\eta \equiv \cos\theta$ and all the metric coefficients are evaluated at $r = r^d_\pm$, which is indeed a function of the polar angle $\theta$ (so that $dr$ has been related to $d\eta$).

Following a standard procedure [21,22], consider the flat-space line element written in spherical-like coordinates,

$$^{(3)}ds^2 = dX^2 + dY^2 \pm dZ^2, \tag{29}$$

where the plus sign refers to the Euclidean case and the minus sign to the Minkowskian case. For the embedding surface in the parametric form

$$X = F(\eta)\cos\phi, \qquad Y = F(\eta)\sin\phi, \qquad Z = G(\eta), \tag{30}$$

the corresponding line element becomes

$$^{(2)}ds^2 = \left[\left(\frac{dF}{d\eta}\right)^2 \pm \left(\frac{dG}{d\eta}\right)^2\right]d\eta^2 + F^2d\phi^2. \tag{31}$$

Comparison with (28) implies

$$\left(\frac{dF}{d\eta}\right)^2 \pm \left(\frac{dG}{d\eta}\right)^2 = h_{\eta\eta}, \qquad F = \sqrt{g_{\phi\phi}}. \tag{32}$$

The relation $F = F(\eta)$ is already given by the second equation and one can then numerically integrate the first equation to get the function $G(\eta)$:

$$G_\pm(\eta) = \int_{\eta_0}^{\eta}\sqrt{\pm\left(h_{\eta\eta} - \left[\frac{d}{d\eta}(\sqrt{g_{\phi\phi}})\right]^2\right)}d\eta, \tag{33}$$

with the initial condition $G(\eta_0) = 0$. Note that the dyadotorus is embeddable entirely in the Euclidean 3-space, whereas the embedding of the outer horizon may become Minkowskian depending on the values of the charge and rotation parameters of the black hole [21]. In the latter case the embedding cross section has a horizontal tangent line when the signature switch of sign in Eq. (33) takes place at a certain value of $\eta$ given by $\eta = \eta_{(ss)}$, where $dG/d\eta = 0$. The integration must be performed with the plus sign (into the Euclidean part of the embedding) or with the minus sign (into the Minkowskian part of the embedding) starting from such a signature-switch point with the initial condition $G(\eta_{(ss)}) = 0$.

Figure 7 shows the embedding diagram of the dyadotorus for the same choice of parameters as in Figs. 4 and 6 as concerns Figs. 7(a), 7(c), and 7(d). Figure 7(b) corresponds instead to a slightly different choice of the charge parameter, satisfying Eq. (22) with the equality sign (implying $\theta^* = 0$), i.e. to the limiting value of $k$ such that the dyadotorus still appears as a toruslike surface, the two branches $r^d_\pm$ still joining (at $\theta = 0,\ \pi$). Despite the appearance the cusps on the axis do not correspond to conical singularities at the axis ($\theta = 0,\ \pi$), as it occurs in contrast in the case of the ergosphere [22,23]. In fact, expanding the induced metric (28) about $\theta = 0$ (or equivalently $\theta = \pi$) to the second order, we get the approximate metric (up to an ignorable constant factor)

$$^{(2)}ds^2 \simeq d\theta^2 + \theta^2d\phi^2 \tag{34}$$

with $\phi \in [0, 2\pi]$, which is the intrinsic metric of a right cone with no deficit angle.

The projections on the $X - Z$ plane of the embedding diagrams of Fig. 7 are shown in Fig. 8.

## V. ON THE ENERGY OF THE DYADOREGION

The total electromagnetic energy distributed in a stationary spacetime can be determined by evaluating the conserved Killing integral (see e.g. [15])

$$E(\xi) = \int_\Sigma T^{(em)}_{\mu\nu}\xi^\mu d\Sigma^\nu, \tag{35}$$

where $\xi = \partial_t$ is the timelike Killing vector, $T^{(em)}_{\mu\nu}$ is the electromagnetic energy-momentum tensor of the source, and $d\Sigma^\nu = n^\nu d\Sigma$ is the surface element vector with $n$ the unit timelike normal to the smooth compact spacelike hypersurface $\Sigma$. The integration is meant to be performed through the whole spacetime occupied by the electromagnetic field, i.e. by allowing $\Sigma$ to extend up to the spatial infinity. Evaluating the electromagnetic energy stored inside a finite region with boundary $r = $ const of spacetime would require instead the introduction of the concept of "quasilocal energy." However, it is interesting to compare the results of the quasilocal treatment with the expression of the electromagnetic energy contained in the portion of spacetime with boundary $r = $ const obtained simply by truncating the integration over $r$ at a given $R$ in Eq. (35):

$$\begin{aligned}E(\xi)_{(r_+, R)} &= \int_{r_+}^R \int_0^\pi \int_0^{2\pi} \mathcal{E}(\xi)\sqrt{h_n}drd\theta d\phi \\ &= \frac{Q^2}{4r_+}\left(1 - \frac{r_+}{R}\right) + \frac{Q^2}{4r_+}\left[\left(1 + \frac{a^2}{r_+^2}\right)\right. \\ &\quad \times \frac{\arctan(a/r_+)}{a/r_+} - \frac{r_+}{R}\left(1 + \frac{a^2}{R^2}\right) \\ &\quad \left. \times \frac{\arctan(a/R)}{a/R}\right], \end{aligned} \tag{36}$$
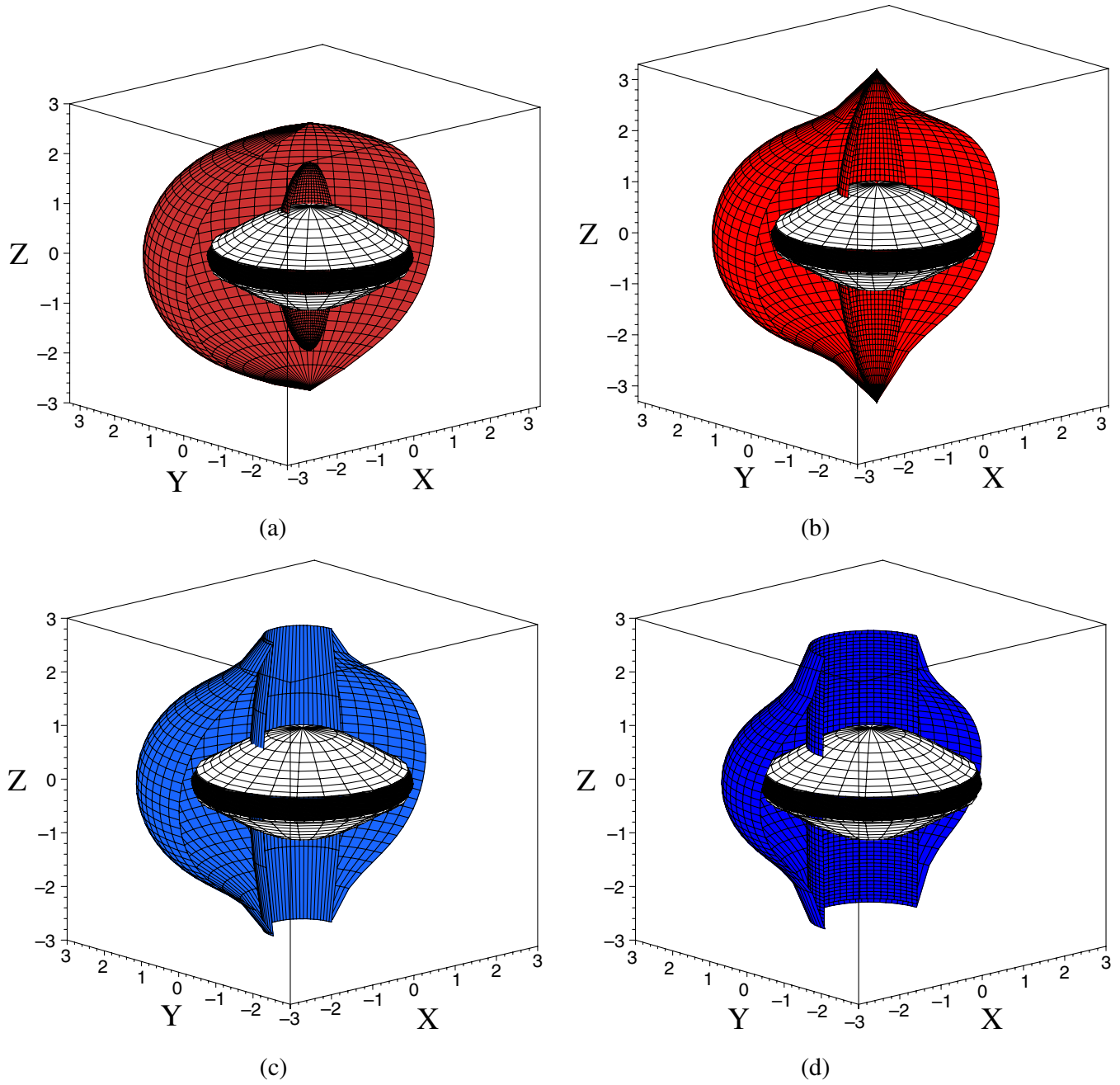
where

FIG. 7 (color online). The dyadotorus is shown on an embedding diagram. The choice of the parameters is the same as in Fig. 4 as concerns (a), (c), and (d). In the case of (b) the value of the parameter $k$ has been changed to the critical value $k \approx 0.998$ in order to satisfy the condition (22) with the equality sign, so representing the limiting case in which the dyadotorus still appears as a toruslike surface [as in (c) and (d)] for the chosen values of parameters $\mu$ and $\alpha$. The surfaces have been cut in half for a better view of the interior, where the embedding of the horizon is also shown (the black shaded region is Euclidean, whereas the white regions are Minkowskian). Note that in this case the coordinates $(X, Y, Z)$ are given by Eq. (30).

$$
\begin{aligned}
\mathcal{E}(\xi) &= T^{(\mathrm{em})}_{\mu\nu}\xi^\mu n^\nu \\
&= \frac{Q^2}{8\pi\Sigma^{5/2}}\sqrt{\Delta}\,\frac{r^2 - a^2\cos^2\theta + 2a^2}{\sqrt{(r^2 + a^2)^2 - \Delta a^2\sin^2\theta}}
\end{aligned}
\tag{37}
$$

can be interpreted as the electromagnetic energy density, $n$

is the unit normal to the time coordinate hypersurfaces, and $h_n = (\Sigma/\Delta)[(r^2 + a^2)^2 - \Delta a^2\sin^2\theta]\sin^2\theta$ is the determinant of the induced metric. It is interesting to note that the same results can be obtained by using the theory of pseudotensors [18] (see Appendix B). In the limit of vanishing rotation parameter Eq. (36) becomes
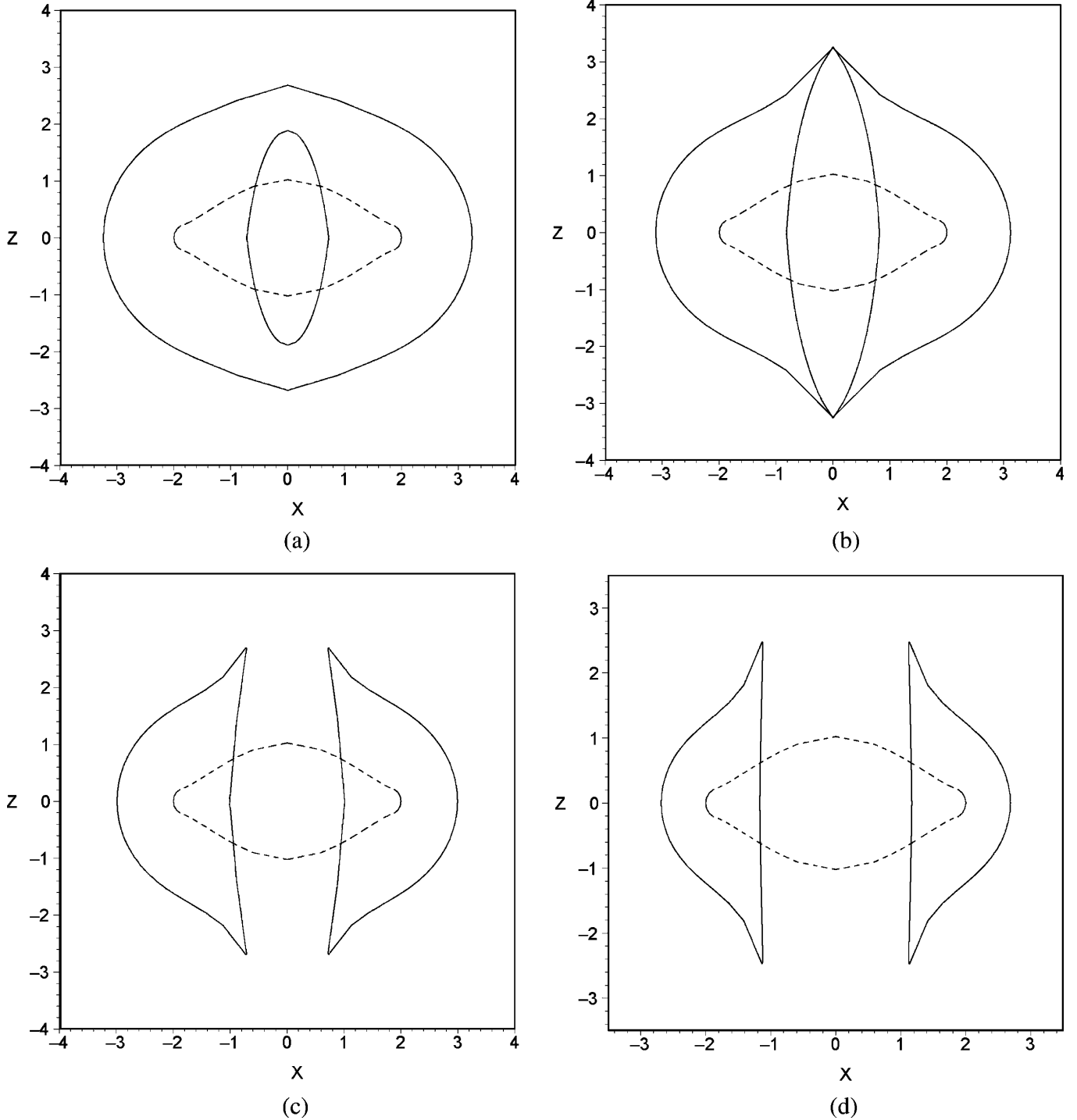
(a)

(b)

(c)

(d)

FIG. 8.   The projections on the $X - Z$ plane of the embedding diagrams of Fig. 7 are shown. Dashed lines correspond to the Minkowskian part of the embedding of the outer horizon.

$$E(\xi)_{(r_+, R)} = \frac{Q^2}{2r_+}\left(1 - \frac{r_+}{R}\right), \qquad (38)$$

which is just the expression for the electromagnetic energy obtained by Vitagliano and Ruffini [15] for the Reissner-Nordström geometry. Equation (35) can be actually con-

sidered as a possible quasilocal definition of energy [24], although it strongly depends on the existence of certain spacetime symmetries, i.e. the existence of a timelike Killing vector, which characterizes stationary spacetimes. In addition, we can see that since the current $J^\mu(\xi) = T^\mu_{(em)\nu}\xi^\nu$ is a conserved vector, the resulting energy does

not depend on the chosen cut through spacetime. In contrast, in any given spacetime one can always introduce a physically motivated congruence of observers $U$ measuring the energy irrespective of spacetime symmetries. But the current $J^\mu(U) = T^\mu_{(em)\nu} U^\nu$ is not a conserved vector in general. Therefore, in this case the energy has an observer dependent meaning; in addition, the results of the measurement could be different for different cuts through spacetime.

Such an approach consists of using the definition [16,17]

$$E_\Sigma(U) = \int_\Sigma T^{(em)}_{\mu\nu} U^\mu d\Sigma^\nu, \qquad (39)$$

where $\Sigma$ is now a bounded hypersurface containing only a finite portion of spacetime, and $U$ is the 4-velocity of the observer measuring the energy. In general, the flux integral of the current $J^\mu(U) = T^\mu_{(em)\nu} U^\nu$ depends on the hypersurface, because this is not connected with the spacetime symmetries. In particular, the vector field $U$ can be chosen to be the unit timelike normal $n$ of $\Sigma$. Therefore, generally we may always evaluate $E_\Sigma(U)$ with respect to any preferred observer $U$, but should not expect to get an answer independent of the chosen cut. In the case of axially symmetric spacetimes in practice there is normally a good time coordinate such as Boyer-Lindquist in Kerr and cuts are chosen to be at constant time. The current $J^\mu(U)$ will be conserved both for static observers and zero angular momentum observers (ZAMOs), since their 4-velocities are aligned with Killing vectors.

Because of the spacetime symmetries it is indeed quite natural to consider in the Kerr-Newman spacetime two families of observers which are described by two geometrically motivated congruences of curves: (1) static observers, at rest at a given point in the spacetime, whose 4-velocity $m = 1/\sqrt{g_{tt}}\partial_t$ is aligned with the Killing temporal direction; (2) ZAMOs, a family of locally nonrotating observers with 4-velocity $n = N^{-1}(\partial_t - N^\phi\partial_\phi)$, where $N = (-g^{tt})^{-1/2}$ and $N^\phi = g_{t\phi}/g_{\phi\phi}$ are the lapse and shift functions respectively, characterized as that normalized linear combination of the two given Killing vectors which is orthogonal to $\partial_\phi$ and future pointing, and it is the unit normal to the time coordinate hypersurfaces. Since the static observers do not exist inside the ergosphere, the ZAMOs seem to be the best candidates to construct the energy (39). However, their 4-velocity diverges at the horizon, since the lapse function goes to zero there.

In order to obtain a finite energy at the horizon, one can then choose a family of infalling observers as the Painlevé-Gullstrand observers, which move radially with respect to ZAMOs and form a congruence of geodesic and irrotational orbits, whose 4-velocity is given by $U_{PG} = N^{-1}(n - \sqrt{1 - N^2}e_{\hat{r}})$. Since they do not follow the spacetime symmetries the current $J^\mu(U_{PG}) = T^\mu_{(em)\nu} U^\nu_{PG}$ is not conserved, so the corresponding energy $E_\Sigma(U_{PG})$ depends on the

hypersurface. The result is that the expression (36) of the electromagnetic energy contained in the dyadoregion constructed by means of the (not normalized) timelike Killing vector agrees with the electromagnetic energy assessed by the Painlevé-Gullstrand geodesic family of infalling observers through the $T = $ const cut of the Kerr-Newman spacetime, where $T$ denotes the Painlevé-Gullstrand time coordinate, i.e.

$$E_\Sigma(\xi) \equiv \underbrace{\int_\Sigma T^{(em)}_{\mu\nu} \xi^\mu d\Sigma^\nu}_{\text{BL coordinates, Killing vector, } t=\text{const cut}}$$

$$= \underbrace{\int_\Sigma T^{(em)}_{\mu\nu} \mathcal{N}^\mu d\Sigma^\nu}_{\text{PG coordinates, PG 4-velocity, } T=\text{const cut}} \equiv E_\Sigma(\mathcal{N}), \qquad (40)$$

with $\mathcal{N}$ the timelike normal to the chosen cut. Details can be found in Appendix B.

From Eq. (36), a rough estimate of the electromagnetic energy stored inside the "dyadoregion" turns out to be given by $E(\xi)_{(r_+, R)} \approx 5.5 \times 10^{-3}$ cm $\approx 6.7 \times 10^{46}$ ergs by assuming $R = 2r_+$ with the same parameters as in Fig. 4(d), and $E(\xi)_{(r_+, R)} \approx 1.9 \times 10^{-2}$ cm $\approx 2.3 \times 10^{47}$ ergs if $R = 3r_+$ with the same choice of parameters as in Fig. 4(a). We note that an exact analytic expression for the electromagnetic energy can also be obtained by taking the actual shape $r = r^d_\pm$ given by Eq. (20) instead of the approximate expression $r = R = $ const in the evaluation of the integral (36). However, this only complicates matters by introducing a nontrivial dependence on the polar angle $\theta$ which makes the integration procedure more involved, even if it can be analytically performed (not shown here for the sake of brevity). Furthermore, the numerical values of the energy corresponding to the above choice of parameters agree with previous estimates.

It is interesting to compare the electromagnetic energy (36) of an extreme Kerr-Newman black hole contained in the portion of spacetime with boundary $R = $ const and that of a Reissner-Nordström black hole (38) with the same total mass and charge in the limit of small charge to mass ratio. In this limit we have

$$E_{RN} \simeq \frac{Q^2}{4M}\left(1 - \frac{2M}{R}\right),$$

$$E_{KN} \simeq \frac{Q^2}{4M}\left(1 - \frac{2M}{R}\right) \qquad (41)$$

$$+ \frac{Q^2}{4M}\left[\frac{\pi}{2} + \frac{M}{R} - \left(1 + \frac{M^2}{R^2}\right)\arctan(M/R)\right].$$

A comparison between energies is meaningful only at infinity, where the radial coordinates of a Kerr-Newman and a Reissner-Nordström geometry can be identified (both with an ordinary radial coordinate in flat space). For $R \to \infty$ we thus have

$$E_{KN} - E_{RN} \rightarrow \frac{Q^2}{4M} \frac{\pi}{2} > 0. \tag{42}$$

## VI. CONCLUSIONS

Vacuum polarization processes can occur in the field of a Kerr-Newman black hole inside a region we have called dyadotorus, whose properties have been investigated here. Such a region has an invariant character, i.e. its existence does not depend on the observer measuring the electromagnetic field: therefore, it is a true physical region.

Some pictorial representations of the boundary surface similar to those commonly used in the literature have been shown employing Cartesian-like coordinates (i.e. ordinary spherical coordinates built up simply using the Boyer-Lindquist radial and angular coordinates) as well as Kerr-Schild coordinates. The dyadotorus has been also shown on the corresponding embedding diagram, which gives the correct geometry allowing to visualize the spacetime curvature.

We have then estimated the electromagnetic energy contained in the dyadotorus by using three different approaches, which give rise to the same final expression for the energy. The first one follows the standard approach consisting of using the (not normalized) timelike Killing vector through the Boyer-Lindquist constant time cut of the Kerr-Newman spacetime (see e.g. [15]), the second one follows a recent observer dependent definition by Katz, Lynden-Bell, and Bičák [16,17] for axially symmetric asymptotically flat spacetimes, for which we have used the Painlevé-Gullstrand geodesic family of infalling observers through the Painlevé-Gullstrand constant time cut, and the last one adopts the pseudotensor theory (see e.g. [18]). We have found by rough estimates that the extreme Kerr-Newman black hole leads to larger values of the electromagnetic energy as compared with a Reissner-Nordström black hole with the same total mass and charge.

It is appropriate to recall that the release of energy via the electron-positron pairs in the dyadotorus is the most powerful way to extract energy from black holes and in all senses corresponds to a new form of energy: the "blackholic" energy [4]. This is a new form of energy different from the traditional ones known in astrophysics. The thermonuclear energy has been recognized to be an energy source of main sequence stars lasting for $10^9$ years [25], the gravitational energy released by accretion processes in neutron stars and black holes has explained the energy observed in binary x-ray sources on time scales $10^6$–$10^8$ years [26]. The blackholic energy appears to be an energy source for the most transient and most energetic events in the universe, the GRBs [4].

## ACKNOWLEDGMENTS

## APPENDIX A: NEWMAN-PENROSE QUANTITIES AND INVARIANT DEFINITION OF THE DYADOTORUS

The existence of the dyadotorus has an invariant character. This fact appears more evident if the electric and magnetic field strengths are expressed in terms of the electromagnetic invariants. Let us adopt here the metric signature $(+, -, -, -)$ in order to use the Newman-Penrose formalism in its original form and then easily get the necessary physical quantities [27,28]. The Kerr-Newman metric is thus given by

$$ds^2 = \left(1 - \frac{2Mr - Q^2}{\Sigma}\right)dt^2 + \frac{2a\sin^2\theta}{\Sigma}(2Mr - Q^2)dtd\phi$$
$$- \frac{\Sigma}{\Delta}dr^2 - \Sigma d\theta^2$$
$$- \left[r^2 + a^2 + \frac{a^2\sin^2\theta}{\Sigma}(2Mr - Q^2)\right]\sin^2\theta d\phi^2, \tag{A1}$$

with associated electromagnetic field

$$F = \frac{Q}{\Sigma^2}(r^2 - a^2\cos^2\theta)dr \wedge [dt - a\sin^2\theta d\phi]$$
$$+ 2\frac{Q}{\Sigma^2}ar\sin\theta\cos\theta d\theta \wedge [(r^2 + a^2)d\phi - ad\phi]. \tag{A2}$$

Introduce the standard Kinnersley principal tetrad [29]

$$l^\mu = \frac{1}{\Delta}[r^2 + a^2, \Delta, 0, a],$$
$$n^\mu = \frac{1}{2\Sigma}[r^2 + a^2, -\Delta, 0, a], \tag{A3}$$
$$m^\mu = \frac{1}{\sqrt{2}(r + ia\cos\theta)}\left[ia\sin\theta, 0, 1, \frac{i}{\sin\theta}\right],$$

which gives nonvanishing spin coefficients

$$\rho = -\frac{1}{r - ia\cos\theta}, \qquad \tau = -\frac{ia}{\sqrt{2}}\rho\rho^*\sin\theta,$$
$$\beta = -\frac{\rho^*}{2\sqrt{2}}\cot\theta, \qquad \pi = \frac{ia}{\sqrt{2}}\rho^2\sin\theta,$$
$$\mu = \frac{1}{2}\rho^2\rho^*\Delta, \qquad \gamma = \mu + \frac{1}{2}\rho\rho^*(r - M),$$
$$\alpha = \pi - \beta^*, \tag{A4}$$

and the only nonvanishing Weyl scalar

$$\psi_2 = M\rho^3 + Q^2\rho^*\rho^3, \tag{A5}$$

showing clearly the Petrov type D nature of the Kerr-Newman spacetime, whereas the Maxwell scalars are

$$\phi_0 = \phi_2 = 0, \qquad \phi_1 = \frac{Q}{2}\rho^2. \tag{A6}$$

The electromagnetic invariants are given by

$$\mathcal{F} \equiv \tfrac{1}{4}F_{\mu\nu}F^{\mu\nu} = \tfrac{1}{2}(\mathbf{B}^2 - \mathbf{E}^2) = 2\,\mathrm{Re}(\phi_0\phi_2 - \phi_1^2),$$
$$\mathcal{G} \equiv \tfrac{1}{4}F_{\mu\nu}{}^*F^{\mu\nu} = \mathbf{E}\cdot\mathbf{B} = -2\,\mathrm{Im}(\phi_0\phi_2 - \phi_1^2), \qquad (A7)$$

where $\mathbf{E}$ and $\mathbf{B}$ are the electric and magnetic fields. Requiring parallel electric and magnetic fields [3] as measured by the Carter observer [20], the previous relations become

$$|\mathbf{B}|^2 - |\mathbf{E}|^2 = -4\,\mathrm{Re}(\phi_1^2), \qquad |\mathbf{E}||\mathbf{B}| = 2\,\mathrm{Im}(\phi_1^2), \qquad (A8)$$

taking into account Eq. (A6). This system can then be easily solved for the magnitudes of $\mathbf{E}$ and $\mathbf{B}$ in the Kerr-Newman background, which turn out to be given by

$$|\mathbf{E}| = |\frac{Q}{\Sigma^2}(r^2 - a^2\cos^2\theta)|, \qquad |\mathbf{B}| = |2\frac{Q}{\Sigma^2}ar\cos\theta|, \qquad (A9)$$

which coincide with those of Eq. (18). We have thus recovered the results by Damour and Ruffini [3], but using a different faster derivation using the Newman-Penrose formalism.

Finally, the Schwinger formula for the rate of pair creation per unit four-volume in terms of the electromagnetic invariants (A7) is given by [13]

$$2\,\mathrm{Im}\mathcal{L} = \frac{e^2|\mathcal{G}|}{4\pi^2\hbar^2}\sum_{n=1}^{\infty}\frac{1}{n}\coth\left\{n\pi\left[\frac{(\mathcal{F}^2+\mathcal{G}^2)^{1/2}+\mathcal{F}}{(\mathcal{F}^2+\mathcal{G}^2)^{1/2}-\mathcal{F}}\right]\right\}$$
$$\times e^{-n\pi E_c/[(\mathcal{F}^2+\mathcal{G}^2)^{1/2}-\mathcal{F}]^{1/2}}. \qquad (A10)$$

After introducing the Carter frame (15) and (16) with respect to which electric and magnetic fields are parallel, the previous formula reduces to Eq. (19), since

$$[(\mathcal{F}^2+\mathcal{G}^2)^{1/2}+\mathcal{F}]^{1/2} = |\mathbf{B}|,$$
$$[(\mathcal{F}^2+\mathcal{G}^2)^{1/2}-\mathcal{F}]^{1/2} = |\mathbf{E}|, \qquad |\mathcal{G}| = |\mathbf{E}||\mathbf{B}|. \qquad (A11)$$

## APPENDIX B: ELECTROMAGNETIC ENERGY USING PAINLEVÉ-GULLSTRAND OBSERVERS AND PSEUDOTENSOR THEORY

In order to evaluate the energy $E_\Sigma(U_{\mathrm{PG}})$ it is useful to transform the Kerr-Newman metric (13) from Boyer-Lindquist coordinates $(t, r, \theta, \phi)$ to Painlevé-Gullstrand coordinates $(T, R, \Theta, \Phi)$ [30,31], which are related by the transformation

$$T = t - \int^r f(r)dr, \qquad R = r, \qquad \Theta = \theta,$$
$$\Phi = \phi - \int^r \frac{a}{r^2 + a^2}f(r)dr, \qquad (B1)$$

where

$$f(r) = -\frac{\sqrt{(2Mr - Q^2)(r^2 + a^2)}}{\Delta}. \qquad (B2)$$

Let us notice that $r$ and $R$ are identified. This is also true for their differential $dr = dR$ but it is no more true for the associated differentiations $\partial_r \neq \partial_R$. Hereafter we will always use $r$ in place of $R$, except for the differentiation operations. In differential form, this transformation writes as

$$dT = dt - f(r)dr, \qquad dR = dr, \qquad d\Theta = d\theta,$$
$$d\Phi = d\phi - \frac{a}{r^2 + a^2}f(r)dr. \qquad (B3)$$

Finally, the Kerr-Newman metric in the Painlevé-Gullstrand coordinates is given by

$$ds^2 = -\left(1 - \frac{2Mr - Q^2}{\Sigma}\right)dT^2 + 2\sqrt{\frac{2Mr - Q^2}{r^2 + a^2}}dTdr$$
$$- \frac{2a(2Mr - Q^2)}{\Sigma}\sin^2\theta dTd\Phi$$
$$+ \sin^2\theta\left[r^2 + a^2 + \frac{a^2(2Mr - Q^2)}{\Sigma}\sin^2\theta\right]d\Phi^2$$
$$- 2a\sin^2\theta\sqrt{\frac{2Mr - Q^2}{r^2 + a^2}}drd\Phi + \frac{\Sigma}{r^2 + a^2}dr^2 + \Sigma d\theta^2, \qquad (B4)$$

with associated electromagnetic field

$$F = \frac{Q}{\Sigma^2}(r^2 - a^2\cos^2\theta)dr \wedge [dT - a\sin^2\theta d\Phi]$$
$$+ 2\frac{Q}{\Sigma^2}ar\sin\theta\cos\theta d\theta \wedge [(r^2 + a^2)d\Phi - adT], \qquad (B5)$$

which has the same form as (14) with $dt \to dT$ and $d\phi \to d\Phi$.

The limit of vanishing rotation parameter $a = 0$ of the previous equations (B4) and (B5) gives rise to the Reissner-Nordström solution in Painlevé-Gullstrand coordinates:

$$ds^2 = -\left(1 - \frac{2M}{r} + \frac{Q^2}{r^2}\right)dT^2 + 2\frac{\sqrt{2Mr - Q^2}}{r}dTdr$$
$$+ dr^2 + r^2(d\theta^2 + \sin^2\theta d\phi^2),$$
$$F = \frac{Q}{r^2}dr \wedge dT. \qquad (B6)$$

In the Painlevé-Gullstrand coordinates the slicing observers ($T$-slicing hereafter) have 4-velocity

$$\mathcal{N} = \partial_T - \frac{\sqrt{(2Mr - Q^2)(r^2 + a^2)}}{\Sigma}\partial_R \qquad (B7)$$

and associated 1-form $\mathcal{N}^\flat = -dT$. This family of $T$-slicing-adapted observers does not coincide with the

$t$-slicing-adapted observers in Boyer-Lindquist coordinates once the coordinate transformation is performed. In fact, when expressed in Boyer-Lindquist coordinates the $T$-slicing-adapted observers move with respect to the $t$-slicing-adapted observers in the radial direction, as already pointed out in Sec. V.

We are now ready to evaluate the energy (39) through a $T = $ const hypersurface as measured by Painlevé-Gullstrand observers with 4-velocity (B7). The energy density turns out to be

$$\mathcal{E}(\mathcal{N}) = T_{\mu\nu}^{(\text{em})} \mathcal{N}^\mu \mathcal{N}^\nu = \frac{Q^2}{8\pi\Sigma^3}(r^2 - a^2\cos^2\theta + 2a^2),$$
(B8)

where $T_{\mu\nu}^{(\text{em})}$ is the Kerr-Newman electromagnetic energy-momentum tensor expressed in Painlevé-Gullstrand coordinates. Let us assume that the boundary $S$ of $\Sigma$ be the 2-surface $r = R = $ const for simplicity. Therefore the energy (39) turns out to be given by

$$E(\mathcal{N})_{(r_+,R)} = 2\pi \int_{r_+}^R \int_0^\pi \mathcal{E}(\mathcal{N})\sqrt{h_\mathcal{N}} dr d\theta$$

$$= -\frac{Q^2}{4a}\left[\frac{a}{r} + \frac{r^2 + a^2}{r^2} \arctan\frac{a}{r} - \frac{\pi}{2}\right]_{r_+}^R$$

$$= \frac{Q^2}{4r_+} - \frac{Q^2}{4R} + \frac{1}{4}\frac{Q^2}{ar_+^2}(r_+^2 + a^2)\arctan\frac{a}{r_+}$$

$$- \frac{1}{4}\frac{Q^2}{aR^2}(R^2 + a^2)\arctan\frac{a}{R},$$
(B9)

where $h_\mathcal{N} = \Sigma^2\sin^2\theta$ is the determinant of the induced metric. The total electromagnetic energy contained in the whole spacetime is obtained by taking the limit $R \to \infty$ in the previous equation:

$$E(\mathcal{N})_{(r_+,\infty)} = \frac{Q^2}{4r_+} + \frac{1}{4}\frac{Q^2}{ar_+^2}(r_+^2 + a^2)\arctan\frac{a}{r_+}, \quad (\text{B10})$$

which in the limiting case $a = 0$ reduces to

$$E^{\text{RN}}(\mathcal{N})_{(r_+,\infty)} = \frac{Q^2}{2r_+}.$$
(B11)

It is interesting to note that the same result (B9) for the energy assessed by Painlevé-Gullstrand observer is achieved simply by using the Killing vector $\xi = \partial_T$, since $\mathcal{E}(\mathcal{N}) = \mathcal{E}(\xi)$. But it is quite surprising that the same result is again obtained by taking a $t = $ const hypersurface in Boyer-Linquist coordinates with unit normal the ZAMO 4-velocity $n$ with respect to "Killing observers" $\xi = \partial_t$ [see Eq. (36)], since

$$\mathcal{E}(\mathcal{N})\sqrt{h_\mathcal{N}} = \mathcal{E}\sqrt{h_n}$$

$$= \frac{Q^2}{8\pi\Sigma^2}(r^2 - a^2\cos^2\theta + 2a^2)\sin\theta. \quad (\text{B12})$$

For completeness we list here similar results presented in Ref. [18] by using the standard definition of symmetric energy-momentum pseudotensor as given by Landau and Lifshitz [32] (LL), although we stress that the physical interpretation of these quantities is controversial in the literature, due to their strict relation with specific coordinate sets. This fact is clearly not in the spirit of general relativity. The LL prescription for the pseudotensor is given by $16\pi L^{\alpha\beta} = \lambda^{\alpha\beta\gamma\delta}{}_{,\gamma\delta}$, where the comma denotes partial derivative and $\lambda^{\alpha\beta\gamma\delta} = -g(g^{\alpha\beta}g^{\gamma\delta} - g^{\alpha\gamma}g^{\beta\delta})$. The conservation law $L^{\alpha\beta}{}_{,\beta} = 0$ implies that the total energy is given by $E = \iiint L^{00}dx^1dx^2dx^3$. By computing the pseudotensor in the quasi-Cartesian Kerr-Schild coordinates previously introduced in Eq. (25) and requiring the integration to be performed on a Boyer-Lindquist $r = R = $ const surface, one obtains the result $E = M - K$, where $K$ is just the rhs of Eq. (B9). Note that in Ref. [18] the same result is obtained using plenty of other different energy-momentum pseudotensors.

[1] R. Ruffini *et al.*, AIP Conf. Proc. **910**, 55 (2007).

[2] R. Ruffini, G. V. Vereshchagin, and S.-S. Xue, Phys. Rep. (to be published).

[3] T. Damour and R. Ruffini, Phys. Rev. Lett. **35**, 463 (1975).

[4] R. Ruffini, in *The Kerr Spacetime: Rotating Black Holes in General Relativity*, edited by D. L. Wiltshire, M. Visser, and S. M. Scott (Cambridge University Press, Cambridge, 2009).

[5] R. Ruffini, in *Proceedings of the Eleventh Marcel Grossmann Meeting on General Relativity*, edited by H. Kleinert, R. T. Jantzen, and R. Ruffini (World Scientific, Singapore, 2008).

[6] R. Ruffini, M. Rotondo, and S.-S. Xue, Int. J. Mod. Phys. D **16**, 1 (2007).

[7] B. Patricelli *et al.*, AIP Conf. Proc. **966**, 143 (2008).

[8] J. A. Rueda H. *et al.*, Bull. Am. Phys. Soc. **53**, 5 (2008), abstract number 8HE.00093.

[9] R. Ruffini, in *Proceedings of the XLIXth Yamada Conference on Black Holes and High-Energy Astrophysics, Tokyo, 1998*, edited by H. Sato and N. Sugiyama (Universal Academy Press, Tokyo, 1998).

[10] G. Preparata, R. Ruffini, and S. S. Xue, Astron. Astrophys. **338**, L87 (1998).

[11] F. Sauter, Z. Phys. **69**, 742 (1931).

[12] W. Heisenberg and H. Euler, Z. Phys. **98**, 714 (1936).

[13] J. Schwinger, Phys. Rev. **82**, 664 (1951).

[14] D. Christodoulou and R. Ruffini, Phys. Rev. D **4**, 3552 (1971).

[15] R. Ruffini and L. Vitagliano, Phys. Lett. B **545**, 233 (2002).

[16] J. Katz, D. Lynden-Bell, and J. Bičák, Classical Quantum Gravity **23**, 7111 (2006).

[17] D. Lynden-Bell, J. Katz, and J. Bičák, Phys. Rev. D **75**, 024040 (2007).

[18] J. M. Aguirregabiria, A. Chamorro, and K. S. Virbhadra, Gen. Relativ. Gravit. **28**, 1393 (1996).

[19] C. W. Misner, K. S. Thorne, and J. A. Wheeler, *Gravitation* (Freeman, San Francisco, 1973).

[20] B. Carter, Commun. Math. Phys. **10**, 280 (1968).

[21] L. Smarr, Phys. Rev. D **7**, 289 (1973).

[22] N. A. Sharp, Can. J. Phys. **59**, 688 (1981).

[23] N. Pelavas, N. Neary, and K. Lake, Classical Quantum Gravity **18**, 1319 (2001).

[24] L. B. Szabados, Living Rev. Relativity **7**, 4 (2004); http://www.livingreviews.org/lrr-2004-4.

[25] H. Bethe, Energy Production in Stars (Nobel Lecture, 1967); http://www.nobelprize.org.

[26] R. Giacconi, The Dawn of X-Ray Astronomy (Nobel Lecture, 2002); http://www.nobelprize.org.

[27] S. Chandrasekhar, *The Mathematical Theory of Black Holes* (Oxford University Press, Oxford, 1983).

[28] D. Bini, C. Cherubini, S. Capozziello, and R. Ruffini, Int. J. Mod. Phys. D **11**, 827 (2002).

[29] W. Kinnersley, J. Math. Phys. (N.Y.) **10**, 1195 (1969).

[30] C. Doran, Phys. Rev. D **61**, 067503 (2000).

[31] G. Cook, Living Rev. Relativity **3**, 5 (2000); http://www.livingreviews.org/lrr-2000-5.

[32] L. D. Landau and E. M. Lifshitz, *The Classical Theory of Fields* (Addison-Wesley, Reading, 1951).

[33] R. Ruffini *et al.*, AIP Conf. Proc. **668**, 16 (2003).